

Neuronal Excitability

# TrkB Signaling Influences Gene Expression in Cortistatin-Expressing Interneurons

 Kristen R. Maynard,<sup>1\*</sup> Alisha Kardian,<sup>1\*</sup> Julia L. Hill,<sup>1</sup> Yishan Mai,<sup>1</sup> Brianna Barry,<sup>1</sup> Henry L. Hallock,<sup>1</sup> Andrew E. Jaffe,<sup>1,2,3,4,5</sup> and  Keri Martinowich<sup>1,4,5</sup>

<https://doi.org/10.1523/ENEURO.0310-19.2019>

<sup>1</sup>Lieber Institute for Brain Development, Johns Hopkins Medical Campus, Baltimore, Maryland 21205, <sup>2</sup>Department of Mental Health, Johns Hopkins University, Baltimore, Maryland 21205, <sup>3</sup>Department of Biostatistics, Johns Hopkins Bloomberg School of Public Health, Baltimore, Maryland 21205, <sup>4</sup>Department of Psychiatry and Behavioral Sciences, Johns Hopkins University School of Medicine, Baltimore, Maryland 21287, and <sup>5</sup>The Solomon H. Snyder Department of Neuroscience, Johns Hopkins University School of Medicine, Baltimore, Maryland 21205

## Abstract

Brain-derived neurotrophic factor (BDNF) signals through its cognate receptor tropomyosin receptor kinase B (TrkB) to promote the function of several classes of inhibitory interneurons. We previously reported that loss of BDNF–TrkB signaling in cortistatin (Cort)-expressing interneurons leads to behavioral hyperactivity and spontaneous seizures in mice. We performed bulk RNA sequencing (RNA-seq) from the cortex of mice with disruption of BDNF–TrkB signaling in cortistatin interneurons, and identified differential expression of genes important for excitatory neuron function. Using translating ribosome affinity purification and RNA-seq, we define a molecular profile for Cort-expressing inhibitory neurons and subsequently compare the transcriptome of normal and TrkB-depleted Cort neurons, revealing alterations in calcium signaling and axon development. Several of the genes enriched in Cort neurons and differentially expressed in TrkB-depleted neurons are also implicated in autism and epilepsy. Our findings highlight TrkB-dependent molecular pathways as critical for the maturation of inhibitory interneurons and support the hypothesis that loss of BDNF signaling in Cort interneurons leads to altered excitatory/inhibitory balance.

**Key words:** ASD; BDNF-TrkB; cortistatin; epilepsy; inhibitory interneurons; Ribotag

## Significance Statement

Mounting evidence suggests that brain-derived neurotrophic factor (BDNF) signals through its receptor TrkB to promote inhibitory interneuron function, including a subpopulation of cortistatin-expressing (Cort) neurons. This study identifies how TrkB depletion in Cort neurons impacts the Cort interneuron transcriptome as well as gene expression in the surrounding cellular milieu of mouse cortex. Our findings highlight TrkB-dependent molecular pathways in the maturation of inhibitory interneurons and further implicate BDNF signaling as critical for regulating excitatory/inhibitory balance. We identified BDNF regulation of a number of genes expressed in Cort neurons that are implicated in both autism and epilepsy, which is of note because these conditions are highly comorbid, and are hypothesized to share underlying molecular mechanisms.

## Introduction

Signaling of brain-derived neurotrophic factor (BDNF) via its transmembrane receptor tropomyosin receptor kinase B (TrkB) plays a significant role in the maturation and

function of inhibitory neurons in the cortex and hippocampus (Yamada et al., 2002; Alcántara et al., 2006). Although inhibitory GABAergic interneurons represent only 10–15% of neurons in the rodent cortex (Meyer et al., 2011), they are highly heterogeneous, differing in morphology,

Received August 1, 2019; accepted December 4, 2019; First published January 13, 2020.

The authors declare no competing financial interest.

Author contributions: K.R.M., J.L.H., and K.M. designed research; K.R.M., A.K., J.L.H., Y.M., B.B., and H.L.H. performed research; K.R.M., A.K., B.B., and A.E.J. analyzed data; K.R.M., A.K., A.E.J., and K.M. wrote the paper.

firing patterns, response to neuromodulators, and molecular profiles (Tremblay et al., 2016). At least 26 different types of GABAergic interneurons have been identified in the hippocampus (Somogyi et al., 2004), and perhaps more in the cerebral cortex (Myers et al., 2007; Habb et al., 2017). Differences in firing properties, connectivity patterns, and molecular expression profiles are hypothesized to contribute to nonoverlapping functions of the respective classes.

BDNF–TrkB signaling plays an important role in the development of several classes of inhibitory interneurons. For example, BDNF regulates the differentiation and morphology of hippocampal interneurons (Marty et al., 1996), and BDNF deletion leads to reduction in several neuropeptide transcripts that define GABAergic populations, including somatostatin (SST), neuropeptide Y (NPY), substance P, and cortistatin (Cort) in the cortex (Glorioso et al., 2006; Martinowich et al., 2011). BDNF decreases the excitability of parvalbumin (Pvalb) interneurons in the dentate gyrus (Nieto-Gonzalez and Jensen, 2013), and accelerates their maturation in the visual cortex (Huang et al., 1999). While BDNF is expressed primarily in excitatory pyramidal neurons, but not in inhibitory interneurons, its receptor TrkB is widely expressed in both excitatory and inhibitory neurons (Cellerino et al., 1996; Gorba and Wahle, 1999; Swanwick et al., 2004). Levels of TrkB expression across different interneuron classes have not been explicitly quantified, but we previously reported that ~50% of Cort-expressing interneurons express TrkB in the cortex (Hill et al., 2019).

Cortistatin is a secreted neuropeptide that is expressed in a distinct set of interneurons. This population partially overlaps with both Pvalb- and SST-expressing inhibitory interneurons, but its expression is seen prominently in the cerebral cortex and hippocampus (de Lecea et al., 1997). Cortistatin is similar in structure to SST and can bind all five cloned somatostatin receptors (Veber et al., 1979; Csaba and Dournaud, 2001). However, Cort possesses some notably distinct functions, including its ability to induce slow-wave sleep activity (de Lecea et al., 1996) and regulated synaptic integration by augmenting the hyperpolarization-activated current  $I_H$  (Schweitzer et al., 2003). Cortistatin is expressed earlier than most inhibitory neuron markers in the brain, peaking at 2 weeks of age in rodents (de Lecea et al., 1997), which closely parallels the pattern of BDNF expression during neurodevelopment

Funding for these studies was provided by the Lieber Institute for Brain Development, the National Institute of Mental Health (Grant R01-MH-105592 to K.M.), and the National Institute of General Medical Sciences (Grant T32-GM-007445 to B.B.).

\*K.R.M. and A.K. contributed equally to this work.

Acknowledgments: We thank the members of the Lieber Institute RNA Sequencing Core, including Joo Heon Shin, Martha Kimos, and Courtney Williams.

Correspondence should be addressed to Keri Martinowich at [Keri.martinowich@libd.org](mailto:Keri.martinowich@libd.org).

<https://doi.org/10.1523/ENEURO.0310-19.2019>

Copyright © 2020 Maynard et al.

This is an open-access article distributed under the terms of the Creative Commons Attribution 4.0 International license, which permits unrestricted use, distribution and reproduction in any medium provided that the original work is properly attributed.

(Kato-Semba et al., 1997). Reductions in BDNF signaling are associated with decreased expression of *Cort* transcripts (Martinowich et al., 2011; Guilloux et al., 2012), and conversely, the administration of cortistatin increases BDNF expression (Souza-Moreira et al., 2013). We previously demonstrated that TrkB expression in Cort interneurons is required to suppress cortical hyperexcitability. Specifically, mice in which TrkB is depleted in Cort interneurons develop spontaneous seizures and die ~1 month after birth. Before developing seizures, these mice sleep for significantly less time and display hyperlocomotion (Hill et al., 2019). While this study established that TrkB signaling in Cort interneurons is critical to maintain appropriate levels of cortical excitability, the molecular mechanisms mediating Cort interneuron dysfunction downstream of TrkB signaling remain known.

To better understand the molecular mechanisms by which BDNF–TrkB signaling influences Cort interneuron development and function, we investigated the impact of TrkB deletion in these cells on the Cort interneuron transcriptome as well as gene expression in the surrounding cellular milieu. Translating ribosome affinity purification (TRAP) has been used to identify molecular profiles for many cell types in the mouse brain, including Cort interneurons (Doyle et al., 2008). Here, we used TRAP to assess how TrkB deletion impacts the molecular profile of these cells, and bulk RNA-sequencing (RNA-seq) to assess how this perturbation affects the surrounding milieu. Using this strategy, we identified several differentially regulated genes, including those encoding molecules important for calcium signaling as well as molecules that influence inhibitory/excitatory balance. Identification of the TrkB-dependent gene pathways that support Cort interneuron function contributes to our understanding of cortical hyperexcitability, which is important because changes in cortical excitability have been implicated in several brain disorders, including epilepsy and autism (Wang et al., 2013; van Diessen et al., 2015).

## Materials and Methods

### Animals

We selectively depleted TrkB in Cort-expressing cells by crossing mice in which Cre-recombinase is expressed under control of the endogenous *Cort* promoter ( $Cort^{tm1(cre)Zjh/J}$ ; referenced in text as *Cort<sup>Cre</sup>*; stock# 010910, The Jackson Laboratory; RRID:IMSR\_JAX:010910; Taniguchi et al., 2011) to mice carrying a *loxP*-flanked TrkB allele (strain fB/fB, referenced in text as *TrkB<sup>fllox/fllox</sup>* (Grishanin et al., 2008; Baydyuk et al., 2011; Hill et al., 2019). *Cort<sup>Cre</sup>* mice were received from The Jackson Laboratory on a mixed C57BL/6J × 129S background. *TrkB<sup>fllox/fllox</sup>* mice were maintained on a C57BL/6J background. *Cort<sup>Cre</sup>* mice were backcrossed to a C57BL/6J background >12X, and *TrkB<sup>fllox/fllox</sup>* mice were backcrossed to a C57BL/6J background before initiating crosses.

For bulk homogenate RNA-seq experiments, the groups were postnatal day 21 (P21) *Cort<sup>Cre</sup>* or *TrkB<sup>fllox/fllox</sup>* (control group contained both genotypes) and *Cort<sup>Cre</sup>*; *TrkB<sup>fllox/fllox</sup>* (experimental group). As seizure onset begins at

P21 (Hill et al., 2019), mice may have developed mild seizures by the time of brain extraction. In all RiboTag experiments, the RiboTag mouse (B6N.129-Rpl22<sup>tm1.1P<sub>sam</sub>/J</sup>; referenced in text as Rpl22<sup>HA</sup>; stock #011029, The Jackson Laboratory; RRID:IMSR\_JAX:011029; Sanz et al., 2009) was used, which expresses a hemagglutinin (HA) tag on the ribosomal protein RPL22 (RPL22<sup>HA</sup>) under control of Cre-recombinase. For RiboTag experiments in Cort neurons, the groups were adult Cort<sup>Cre</sup>; Rpl22<sup>HA</sup> Input versus Cort<sup>Cre</sup>; Rpl22<sup>HA</sup> immunoprecipitation (IP). For RiboTag experiments in TrkB-deleted versus TrkB-intact Cort neurons, the groups were P21 Cort<sup>Cre</sup>; Rpl22<sup>HA</sup> mice and Cort<sup>Cre</sup>; TrkB<sup>flox/flox</sup>; Rpl22<sup>HA</sup> mice (experimental group).

All mice were housed in a temperature-controlled environment with a 12 h light/dark cycle and *ad libitum* access to standard laboratory chow and water. Mice were group housed based on genotype. All experimental animal procedures were approved by the SoBran Biosciences Institutional Animal Care and Use Committee. Male and female mice were included and analyzed for all experiments.

### RNA extraction and quantitative PCR

Mice were cervically dislocated, and cortices were flash frozen in isopentane. For bulk homogenate experiments in P21 control and Cort<sup>Cre</sup>; TrkB<sup>flox/flox</sup> mice, RNA was extracted using Life Technologies TRIzol (Thermo Fisher Scientific), purified using RNeasy minicolumns (Qiagen), and quantified using a Nanodrop spectrophotometer (Agilent Technologies). RNA concentrations were normalized and reversed transcribed using Life Technologies Superscript III (Thermo Fisher Scientific). Quantitative PCR (qPCR) was performed using a Realplex Thermocycler (Eppendorf) with Life Technologies GEMM mastermix (Thermo Fisher Scientific) and 40 ng of synthesized cDNA. Individual mRNA levels were normalized for each well to *Gapdh* mRNA levels. For validation of genes differentially expressed in control and experimental RiboTag samples, cDNA was synthesized using the Ovation RNA Amplification System V2 Kit (described below), and qPCR was performed as above. TaqMan probes were commercially available from Thermo Fisher Scientific (*Gad1* Mm00725661\_s1, *Cort* Mm00432631\_m1, *Gfap* Mm01253033\_m1, *Wt1* Mm01337048\_m1; *Cxcr4* Mm01292123\_m1; *Calb1* Mm00486647\_m1; *Lgals1* Mm00839408\_g1; *Trpc6* Mm01176083\_m1; *Syt6* Mm04932997\_m1; *Gng4* Mm00772342\_m1; *Ttc9b* Mm01176446\_m1; *S100a10* Mm00501458\_g1; *Nxph1* Mm01165166\_m1; and *Syt2* Mm00436864\_m1; *Gsn* Mm00456679\_m1) or as described in the study by Martinovich et al. (2011). Statistical analysis was conducted using GraphPad Prism (GraphPad Software). Comparisons between two groups were performed using unpaired Student's *t* test. Data are presented as the mean ± SEM and statistical significance was set at \**p* < 0.05, \*\**p* < 0.01, \*\*\**p* < 0.001, \*\*\*\**p* < 0.0001.

### RNAscope single-molecule fluorescent *in situ* hybridization

Control and Cort<sup>Cre</sup>; TrkB<sup>flox/flox</sup> P21 mice were cervically dislocated and the brains were removed from the skull, flash frozen in isopentane, and stored at −80°C.

Brain tissue was equilibrated to −20°C in a cryostat (Leica), and serial sections of cortex were collected at 16 μm. Sections were stored at −80°C until completion of the RNAScope assay. We performed single-molecule fluorescent *in situ* hybridization using the RNAScope Fluorescent Multiplex Kit version 2 [catalog #323100, Advanced Cell Diagnostics (ACD)] according to the study by Colliva et al. (2018). Briefly, tissue sections were fixed with a 10% neutral buffered formalin solution (catalog #HT501128, Sigma-Aldrich) for 20 min at room temperature and pretreated with protease for 20 min. Sections were incubated with commercially available *Wt1* (catalog #432711, ACD) and *Cre* (catalog #312281-C2, ACD) probes. Probes were fluorescently labeled with orange (excitation, 550 nm), green (excitation, 488 nm), or far red (excitation, 647) fluorophores using the Amp 4 Alt B-FL. Confocal images were acquired in z-series at 63× magnification using a Zeiss 700LSM confocal microscope. Images were blinded, and transcript colocalization was quantified using custom MATLAB functions. Briefly, cell nuclei were isolated from the DAPI channel using the cellsegm toolbox (Gaussian smoothing, adaptive thresholding, and splitting of oversized segmented nuclei; Hodneland et al., 2013). Once centers and boundaries of individual cells were isolated, an intensity threshold was set for transcript detection, and watershed segmentation was used to split detected pixel clusters in each channel into identified transcripts. Custom MATLAB functions were then used to determine the size of each detected transcript (regionprops3 function in Image Processing toolbox). Each transcript was then assigned to a nucleus based on its position in three dimensions. Transcripts with centers outside the boundaries of a nucleus were excluded from further analysis. A cell was considered to be positive for a gene if more than two transcripts were present.

### Bulk cortex RNA-Seq

Cortices of control (*n* = 5) and Cort<sup>Cre</sup>; TrkB<sup>flox/flox</sup> (*n* = 5) mice were collected and flash frozen in isopentane. RNA was extracted from one hemisphere of each animal using Life Technologies TRIzol (Thermo Fisher Scientific), purified with RNeasy minicolumns (Qiagen), and quantified using Nanodrop. The Nextera XT DNA Library Preparation Kit was used to generate sequencing libraries according to manufacturer instructions. Samples were sequenced on the HiSeq2000 (Illumina).

### RiboTag and RNA-Seq of Cort interneurons

Cortices of Cort<sup>Cre</sup>; Rpl22<sup>HA</sup> mice (*n* = 3) were collected and flash frozen in isopentane. For each sample (*n* = 3 Input, *n* = 3 IP), one hemisphere of the cortex from each animal was homogenized according to previously described protocols (Sanz et al., 2013). An aliquot of homogenate was flash frozen and reserved for “Input” samples. Ribosome-mRNA complexes (“IP” samples) were affinity purified using a mouse monoclonal HA antibody (MMS-101R, Covance; RRID:AB\_2565334) and Pierce A/G magnetic beads (catalog #88803, Thermo Fisher Scientific). RNA from Input and IP samples was purified using RNeasy microcolumns (Qiagen) and quantified using the

**Table 1: Statistics**

Figure	Data structure	Type of test	Type I error control	Notes
1B	Gene counts for differential expression analysis	Moderated <i>t</i> tests with linear regression (empirical Bayes)	FDR < 0.1	limma Bioconductor package: voom approach
1C	Gene set enrichment analysis	Hypergeometric test	FDR < 0.05	clusterProfiler Bioconductor package: compareClusters approach
1D	Normalized qPCR data	Student's <i>t</i> test	$p < 0.05$	
2B	Normalized qPCR data	Student's <i>t</i> test	$p < 0.05$	
2C	Gene counts for differential expression analysis	Moderated <i>t</i> tests with linear mixed effects modeling (empirical Bayes)	Bonferroni < 0.05	limma Bioconductor package: voom approach
2D	Gene set enrichment analysis	Hypergeometric test	FDR < 0.05	clusterProfiler Bioconductor package: compareClusters approach
2E	Normalized qPCR data	Student's <i>t</i> test	$p < 0.05$	
3B	Normalized qPCR data	Student's <i>t</i> test	$p < 0.05$	
3C	Differential expression analysis	Moderated <i>t</i> tests with linear regression (empirical Bayes)	FDR < 0.05	limma Bioconductor package: voom approach
3D	GO enrichment analysis	Hypergeometric test	FDR < 0.05	clusterProfiler Bioconductor package: compareClusters approach
4A	Normalized qPCR data	Student's <i>t</i> test	$p < 0.05$	
4B	Normally distributed	Student's <i>t</i> test	$p < 0.05$	

Invitrogen Ribogreen RNA Assay Kit (catalog #R11490, Thermo Fisher Scientific). Sequencing libraries were prepared using the SMARTer Stranded RNA-Seq Kit (Clontech) and sequenced on the HiSeq2000 (Illumina).

### Ribotag and RNA-Seq of Cort interneurons following disruption of BDNF–TrkB signaling

Cortices of control ( $n = 6$ ) or Cort<sup>Cre</sup>,TrkB<sup>flox/flox</sup>; Rpl22<sup>HA</sup> ( $n = 6$ ) mice were collected and flash frozen in isopentane. One hemisphere of the cortex from each animal was homogenized according to previously described protocols (Sanz et al., 2013). Sixty-five microliters of total homogenate was flash frozen and reserved for Input samples. Ribosome-mRNA complexes (IP samples) were affinity purified using a mouse monoclonal HA antibody (MMS-101R, Covance) and PierceA/G magnetic beads (88803, Thermo Fisher Scientific). RNA from Input and IP samples was purified using RNeasy microcolumns (Qiagen) and quantified using the Invitrogen Ribogreen RNA Assay Kit (R11490 Thermo Fisher Scientific). The Ovation RNA Amplification System V2 Kit (7102, NuGEN) was used to amplify cDNA from 10 ng of RNA according to manufacturer instructions. cDNA was used for qPCR validation for *Cort* enrichment in IP versus Input samples. Sequencing libraries were generated with the Ovation SoLo RNA-seq System Mouse (0502–32, NuGEN) according to manufacturer instructions from 10 ng of RNA. Library concentration was quantified using the KAPA Library Quantification Kit (KR0405, KAPA Biosystems). Libraries were sequenced using the MiSeq Reagent Kit v3 (MS-102–3001, Illumina) and NuGEN Custom SoLo primer.

### RNA-Seq data processing and analyses

RNA-seq reads from all experiments were aligned and quantified using a common processing pipeline. Reads were aligned to the mm10 genome using the HISAT2 splice-aware aligner (Kim et al., 2015), and alignments

overlapping genes were counted using featureCounts version 1.5.0-p3 (Liao et al., 2014) relative to Gencode version M11 (118,925 transcripts across 48,709 genes; March 2016). Differential expression analyses were performed on gene counts using the voom approach (Law et al., 2014) in the limma R/Bioconductor package (Ritchie et al., 2015) using weighted trimmed means normalization factors using the statistical models described below (Table 1). For each analysis, multiple testing correction was performed using the Benjamini–Hochberg approach to control for the false discovery rate (FDR; Kasen et al., 1990). Gene set enrichment analyses were performed on marginally significant genes using the subset of genes with known Entrez gene IDs against a background of all expressed genes using the clusterProfiler R Bioconductor package, which uses the hypergeometric test (Yu et al., 2012).

Cross-species enrichment analyses of the human SFARI (Banerjee-Basu and Packer, 2010) and Harmonizome (Rouillard et al., 2016) gene sets were performed with Fisher exact tests (which is identical to the above hypergeometric test on these  $2 \times 2$  enrichment tables) on the subsets of homologous and expressed genes in each mouse dataset. For SFARI analyses, we considered the sets of (1) all genes in the mouse model database, (2) all genes in the human gene database ( $N = 1079$  genes), (3) only genes that were syndromic or had gene scores of 1 or 2 ( $N = 235$  genes, which correspond to high-confidence genes), and (4) only genes that had gene scores of 1 or 2, ignoring syndromic genes ( $N = 91$  genes). All RNA-seq analysis code is available on GitHub: [https://github.com/Lieber-Institute/cst\\_trap\\_seq](https://github.com/Lieber-Institute/cst_trap_seq). Raw RNA-seq reads are available at BioProject Accession PRJNA602667.

### Bulk cortex analysis for genotype effects

We used paired end read alignment and gene counting for these 10 samples (5 per genotype group). We analyzed

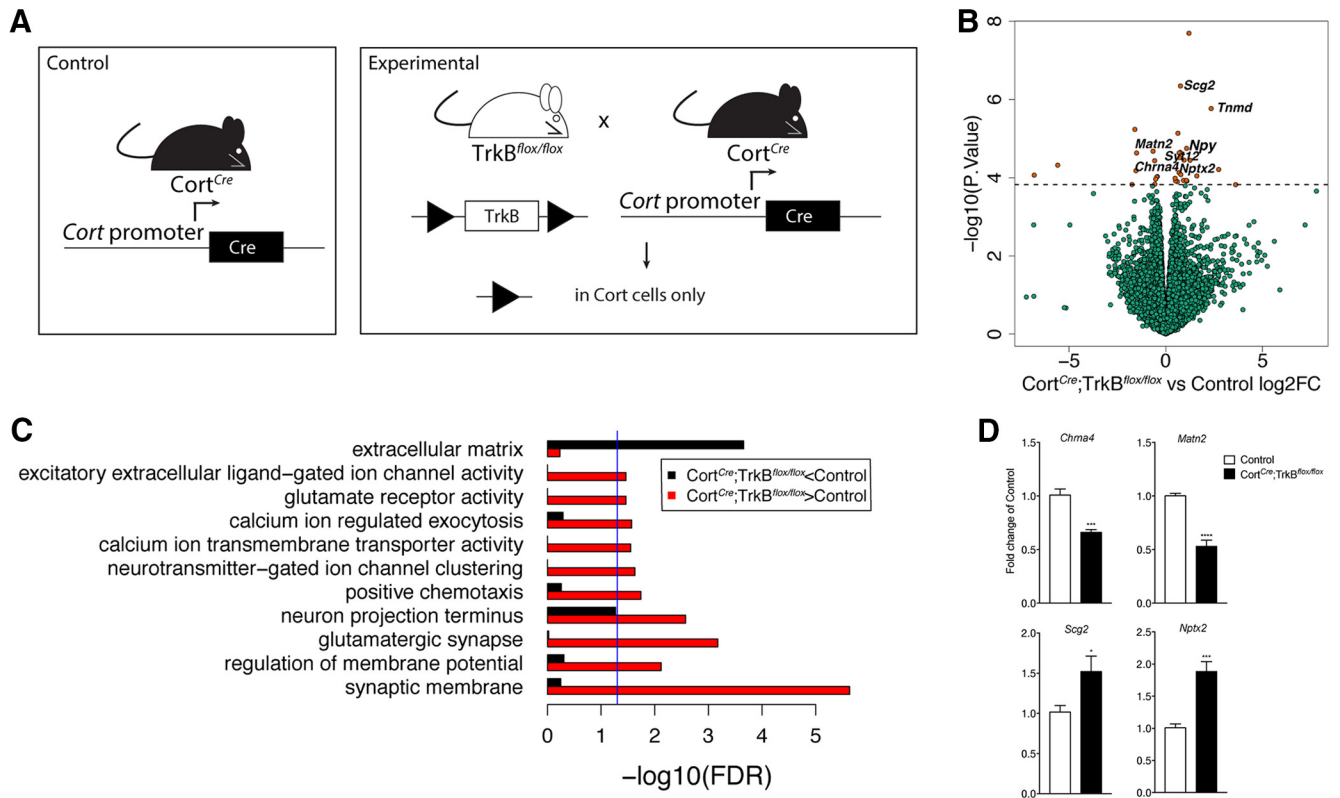


**Figure 1.** Loss of TrkB signaling in Cort interneurons causes gene expression changes in pathways regulating excitability. **A**, Schematic of control and Cort<sup>Cre</sup>;TrkB<sup>flox/flox</sup> mice. **B**, Volcano plot of bulk homogenate RNA-seq results with Cort<sup>Cre</sup>;TrkB<sup>flox/flox</sup> versus Control log<sub>2</sub> fold change against  $-\log_{10} p$  value. Orange dots represent genes that are significantly different in Cort<sup>Cre</sup>;TrkB<sup>flox/flox</sup> versus Control, including *Npy*, *Syt12*, *Nptx2*, and *Chma4*. Green dots represent nonsignificant genes. See Extended Data Figure 1-1. **C**, GO terms in the molecular function, biological processes, and cellular component categories for genes enriched and de-enriched in cortical tissue following ablation of TrkB in Cort neurons. See Extended Data Figure 1-2. **D**, qPCR analysis validating genes found to be differentially expressed in bulk cortical homogenate RNA-seq of Cort<sup>Cre</sup>;TrkB<sup>flox/flox</sup> versus Control mice ( $n = 5$  per genotype, Student's unpaired  $t$  test; data are presented as the mean  $\pm$  SEM: \* $p < 0.05$  \*\*\* $p < 0.001$  \*\*\*\* $p < 0.0001$  vs control).

21,717 genes with reads per kilobase per million counted/assigned (RPKM normalizing to total number of gene counts, not mapped reads)  $> 0.1$ . We performed differential expression analysis with limma voom using genotype as the main outcome of interest, further adjusting for the gene assignment rate (measured by featureCounts), the chrM mapping rate, and one surrogate variable.

**Input versus IP analysis**

We used paired end read alignment and gene counting for these six samples (three input and three IP). We analyzed 21,776 genes with RPKM  $> 0.1$ . We performed differential expression analysis with limma voom using fraction (IP vs Input) as the main outcome of interest, further adjusting for the gene assignment rate (measured by featureCounts) and also using the duplicateCorrelation function in limma to treat each mouse as a random intercept by using linear mixed-effects modeling.

**IP analysis for genotype effects**

We used single end read alignment and gene counting for these 12 samples (6 per genotype). We analyzed 21,187 genes with RPKM  $> 0.1$ . We performed differential expression analysis with limma voom using genotype as the main outcome of interest, further adjusting for the gene assignment rate (measured by featureCounts).

**Results**

**Disruption of BDNF-TrkB Signaling in Cort Interneurons Alters Cortical Gene Expression**

Mice with selective depletion of TrkB in Cort-expressing interneurons (Cort<sup>Cre</sup>;TrkB<sup>flox/flox</sup>; Fig. 1A) develop spontaneous seizures at approximately P21 (Hill et al., 2019). To better understand the molecular mechanisms downstream of TrkB signaling disruption in Cort interneurons that leads to hyperexcitability and disruption of excitatory/inhibitory balance, we performed bulk RNA-seq on the cortices of P21 Cort<sup>Cre</sup>;TrkB<sup>flox/flox</sup> ( $n = 5$ ) and littermate controls ( $n = 5$ ). Among the 21,717 expressed genes (at RPKM  $> 0.1$ ), we identified 33 differentially expressed between Cort<sup>Cre</sup>;TrkB<sup>flox/flox</sup> and controls at FDR  $< 0.1$  including 15 genes with absolute fold changes  $> 2$  (Fig. 1B, Extended data Fig. 1-1). Of particular interest, we observed increased expression of genes involved in cortical excitability such as tenomodulin (*Tnmd*, encoding an angiogenesis inhibitor implicated in Alzheimer's; Tolpanen et al., 2011), *Npy* (encoding a neuropeptide synthesized by GABAergic interneurons; Karagiannis et al., 2009), and calsenilin (*Kcnp3*, encoding a calcium binding protein that influences cortical excitability; Pruunsild and Timmusk, 2005; 5.06-, 1.68-, and 1.52-fold changes, re-

spectively;  $p = 1.7 \times 10^{-6}$ ,  $2.24 \times 10^{-5}$ ,  $1.26 \times 10^{-4}$ ). We also observed decreased expression of ATPase plasma membrane  $\text{Ca}^{2+}$  transporting 4 (*Atp2b4*), matrilin 2 (*Matn2*), and cholinergic receptor nicotinic alpha 4 subunit (*Chrna4*; 1.48-, 1.57-, and 1.49-fold changes, respectively;  $p = 1.46 \times 10^{-4}$ ,  $2.1 \times 10^{-5}$ , and  $3.68 \times 10^{-5}$ , respectively). These genes encode proteins that are important for intracellular calcium homeostasis, formation of filamentous networks in the extracellular matrix, and acetylcholine signaling, respectively (Kuryatov et al., 1997; Mátés et al., 2002; Ho et al., 2015). To independently validate RNA-seq results, we confirmed differential expression of a subset of upregulated and downregulated genes using qPCR. We verified significant elevation of secretogranin II (*Scg2*) and neuronal pentraxin II (*Nptx2*), additional genes of interest due to their roles in packaging neuropeptides into secretory vesicles and excitatory synapse formation, in *Cort<sup>Cre</sup>;TrkB<sup>fllox/fllox</sup>* mice compared with control mice (1.5- and 2-fold changes;  $p < 0.5$  and  $0.001$ , respectively; Fig. 1D; Ozawa and Takata, 1995; O'Brien et al., 1999). We also validated the reduction of *Chrna4* and *Matn2* transcripts (0.6- and 0.5-fold changes,  $p < 0.001$  and  $0.0001$ , respectively; Fig. 1D).

To identify signaling pathways impacted by differentially expressed genes in *Cort<sup>Cre</sup>;TrkB<sup>fllox/fllox</sup>* cortex compared with control, we performed gene ontology (GO) analysis on the subset of 269 marginally significant (at  $p < 0.005$ ) genes with Entrez gene IDs, stratified by directionality (133 more highly expressed in control and 136 more highly expressed in *Cort<sup>Cre</sup>;TrkB<sup>fllox/fllox</sup>*; Fig. 1C, Extended Data Fig. 1-2). Consistent with the hyperexcitability phenotype in *Cort<sup>Cre</sup>;TrkB<sup>fllox/fllox</sup>* mice, analysis with the cellular component category showed terms such as glutamatergic synapse ( $p = 3.69 \times 10^{-5}$ ), neuron projection terminus ( $p = 2.63 \times 10^{-4}$ ), and collagen-containing extracellular matrix ( $p = 3.06 \times 10^{-8}$ ). Analysis with the molecular function category showed terms such as calcium ion transmembrane transporter activity ( $p = 4.75 \times 10^{-4}$ ), glutamate receptor activity ( $p = 1.35 \times 10^{-3}$ ), and excitatory extracellular ligand-gated ion channel activity ( $p = 1.52 \times 10^{-3}$ ). Analysis with the biological processes category showed terms such as positive chemotaxis ( $p = 3.07 \times 10^{-4}$ ), calcium ion-regulated exocytosis ( $p = 6.67 \times 10^{-4}$ ), and neurotransmitter-gated ion channel clustering ( $p = 4.55 \times 10^{-4}$ ). Together, GO analysis of differentially expressed genes supports the hypothesis that the disruption of BDNF–TrkB signaling in Cort interneurons impacts signaling pathways that control excitatory/inhibitory balance and network excitability.

### Translatome profiling delineates a comprehensive molecular identity for Cort-expressing interneurons in the cortex

Given the critical role of Cort neurons in maintaining cortical excitatory/inhibitory balance, we sought to better understand the molecular profile of Cort neurons using TRAP followed by RNA-seq. We first crossed mice expressing Cre recombinase under control of the cortistatin promoter (*Cort<sup>Cre</sup>*) to mice expressing a Cre-dependent HA peptide tag on the RPL22 ribosomal subunit (*Rpl22<sup>HA</sup>*;

Fig. 2A) to allow for HA tagging of ribosomes selectively in Cort neurons. Tagged ribosomes were immunoprecipitated (IP) from cortical homogenate tissue (Input) using an anti-HA antibody. Ribosome-associated RNA was isolated from IP samples and total RNA was isolated from Input samples.

Cell type-specific expression of the RiboTag allele in Cort neurons was confirmed by qPCR analysis showing significant enrichment of *Cort* transcripts in IP compared with the Input fraction (~20-fold;  $p < 0.0001$ ; Fig. 2B). We also showed expected enrichment of glutamate decarboxylase 1 (*Gad1*) and depletion of glial fibrillary acidic protein (*Gfap*) and *Bdnf* exon IV-containing transcripts (6-, 0.25-, and 0.2-fold changes,  $p < 0.01$ ,  $p = 0.0707$ , and  $p = 0.0581$ , respectively; Fig. 2B; Gorba and Wahle, 1999; Swanwick et al., 2004). Having confirmed successful IP from Cort-expressing interneurons, we generated stranded, ribosomal RNA depleted low-input libraries from Input and IP fractions and performed RNA-seq. Among the 21,776 expressed genes (at RPKM > 0.1), we identified 868 differentially expressed between Input and IP RNA fractions at Bonferroni-corrected  $p$  values < 0.05 (and 5362 genes at FDR < 0.05), including 627 genes with absolute fold changes > 2 (Fig. 2C, Extended Data Fig. 2-1). Reassuringly, differential expression analysis confirmed significant enrichment (IP/Input) of *Cort* transcripts (2.7-fold increase,  $p = 3.93 \times 10^{-3}$ ) and significant depletion of transcripts for *Gfap*, *Mal* (T-cell differentiation protein), *Slc25a18* (solute Carrier Family 25 Member 18) and *Bdnf*, genes enriched in astrocytes, oligodendrocytes, and excitatory neurons, respectively (Schaeren-Wiemers et al., 1995b; Zhou and Danbolt, 2014; Hol and Pekny, 2015; Sasi et al., 2017). To independently validate our RNA-seq results, we confirmed differential expression of a subset of enriched and de-enriched genes, including neurexophilin 1 (*Nxph1*), synaptotagmin 2 (*Syt2*), tetratricopeptide repeat domain 9B (*Ttc9b*), and S100 calcium binding protein A10 (*S100a10*). These genes are of particular interest given their role in synapse function and calcium signaling (Pang et al., 2006; Svenningsson et al., 2013). Using qPCR, we verified significant enrichment of *Nxph1* and *Syt2* and de-enrichment of *Ttc9b* and *S100a10* in Cort IP compared with Input samples (7.0-, 7.0-, 0.2-, and 0.1-fold changes, respectively;  $p < 0.0001$ ; Fig. 2E). To further confirm these results, we performed cell type-specific expression analysis (CSEA) on the top 100 differentially expressed genes based on fold change. This analysis confirmed significant over-representation of transcripts expressed in Cort neurons (Extended Data Fig. 2-2; Xu et al., 2014).

To discover the potential functional significance of the mRNAs enriched and depleted in Cort-expressing interneurons in the cortex, we performed GO analysis on the subset of 848 Bonferroni-significant genes differentially expressed in Cort IP compared with Input with Entrez gene IDs, stratified by directionality (440 more highly expressed in IP, 408 more highly expressed in Input; Fig. 2D, Extended Data Fig. 2-3). Genes enriched in IP fractions are involved in cellular component category terms such as axon part and neuron projection terminus and in

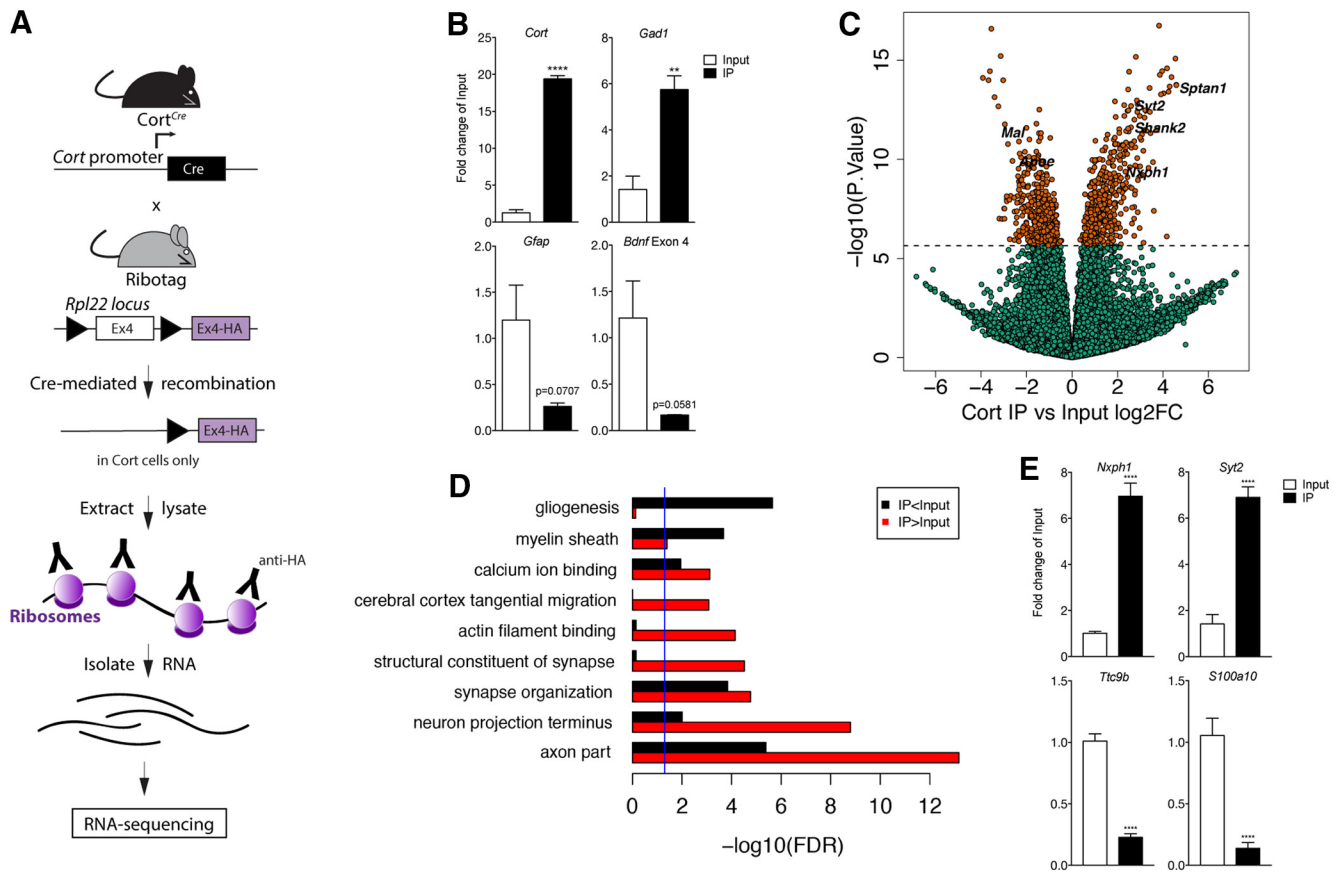


**Figure 2.** Translating ribosome affinity purification defines a unique molecular signature for cortistatin interneurons in the cortex. **A**, Locus of the ribosomal protein Rpl22 in the RiboTag mouse and breeding strategy used to obtain *Cort<sup>Cre</sup>;Rpl22<sup>HA</sup>* mice. Schematic of RiboTag experimental workflow. **B**, Validation of RiboTag allele expression in cortistatin neurons by qPCR for *Cort* as well as *Gad*, *Gfap*, and *Bdnf* exon IV ( $n = 3$  per genotype, Student’s unpaired  $t$  test; data are presented as the mean  $\pm$  SEM:  $***p < 0.01$   $****p < 0.0001$  vs control). **C**, Volcano plot of RNA-seq results with *Cort<sup>Cre</sup>;Rpl22<sup>HA</sup>* Input versus *Cort<sup>Cre</sup>;Rpl22<sup>HA</sup>* IP  $\log_2$  fold change against  $-\log_{10} p$  value. Orange dots represent genes that are significantly different in Input versus IP fractions, including *Syt2*, *Nrx1*, *Mal*, and *ApoE*. Green dots represent nonsignificant genes. See Extended Data Figures 2-1 and 2-2. **D**, GO terms in the molecular function, biological processes, and cellular component categories for genes enriched and de-enriched in Cort-expressing interneurons. See Extended Data Figure 2-3. **E**, qPCR analysis validating genes found to be differentially expressed in Input versus IP RNA sequencing results ( $n = 3$  per genotype, Student’s unpaired  $t$  test; data are presented as the mean  $\pm$  SEM:  $****p < 0.0001$  vs control).

biological process category terms such as synapse organization and cerebral cortex tangential migration. Genes enriched in Input fractions are involved in cellular component category terms such as myelin sheath and biological processes category terms such as gliogenesis. De-enrichment of myelin and gliogenesis pathways would be expected in the neuronal IP fractions, and hence further validate our approach.

**Loss of BDNF–TrkB signaling in Cort interneurons impacts genes critical for structural and functional plasticity**

To better understand signaling pathways and cellular functions modulated by BDNF–TrkB signaling in Cort cells, we performed TRAP followed by RNA-seq in TrkB-depleted Cort interneurons. We intercrossed *Cort<sup>Cre</sup>;Rpl22<sup>HA</sup>* mice to mice expressing a floxed TrkB allele (*TrkB<sup>flox/flox</sup>*) to allow for HA tagging of ribosomes in control Cort interneurons (*Cort<sup>Cre</sup>;Rpl22<sup>HA</sup>*) or TrkB-depleted

Cort interneurons (*Cort<sup>Cre</sup>;TrkB<sup>flox/flox</sup>;Rpl22<sup>HA</sup>*; referred to hereafter as *Cort<sup>Cre</sup>;TrkB<sup>flox/flox</sup>*, Fig. 3A). For control and experimental animals ( $n = 6$  each), tagged ribosomes were selectively immunoprecipitated (IP) from cortical homogenate tissue (Input) using an anti-HA antibody. Ribosome-associated RNA was isolated from IP samples and total RNA was isolated from Input samples.

Cell type-specific expression of the RiboTag allele in Cort interneurons was confirmed by qPCR analysis showing significant enrichment of *Cort* in IP versus Input fractions (12–15-fold;  $p < 0.0001$ ; Fig. 3B). As expected, there was also significant enrichment of *Gad1* (8–12-fold;  $p < 0.001$  for control,  $p < 0.0001$  for *Cort<sup>Cre</sup>;TrkB<sup>flox/flox</sup>* mice; Fig. 3B) and significant depletion of *Gfap* (0.2–0.3-fold;  $p < 0.01$  for both groups; Fig. 3B) and *Bdnf* exon IV-containing transcripts (0.1–0.3-fold;  $p < 0.001$  for control,  $p < 0.05$  for *Cort<sup>Cre</sup>;TrkB<sup>flox/flox</sup>* mice; Fig. 3B). We generated libraries from control and *Cort<sup>Cre</sup>;TrkB<sup>flox/flox</sup>* IP fractions and performed RNA-seq to generate a compre-

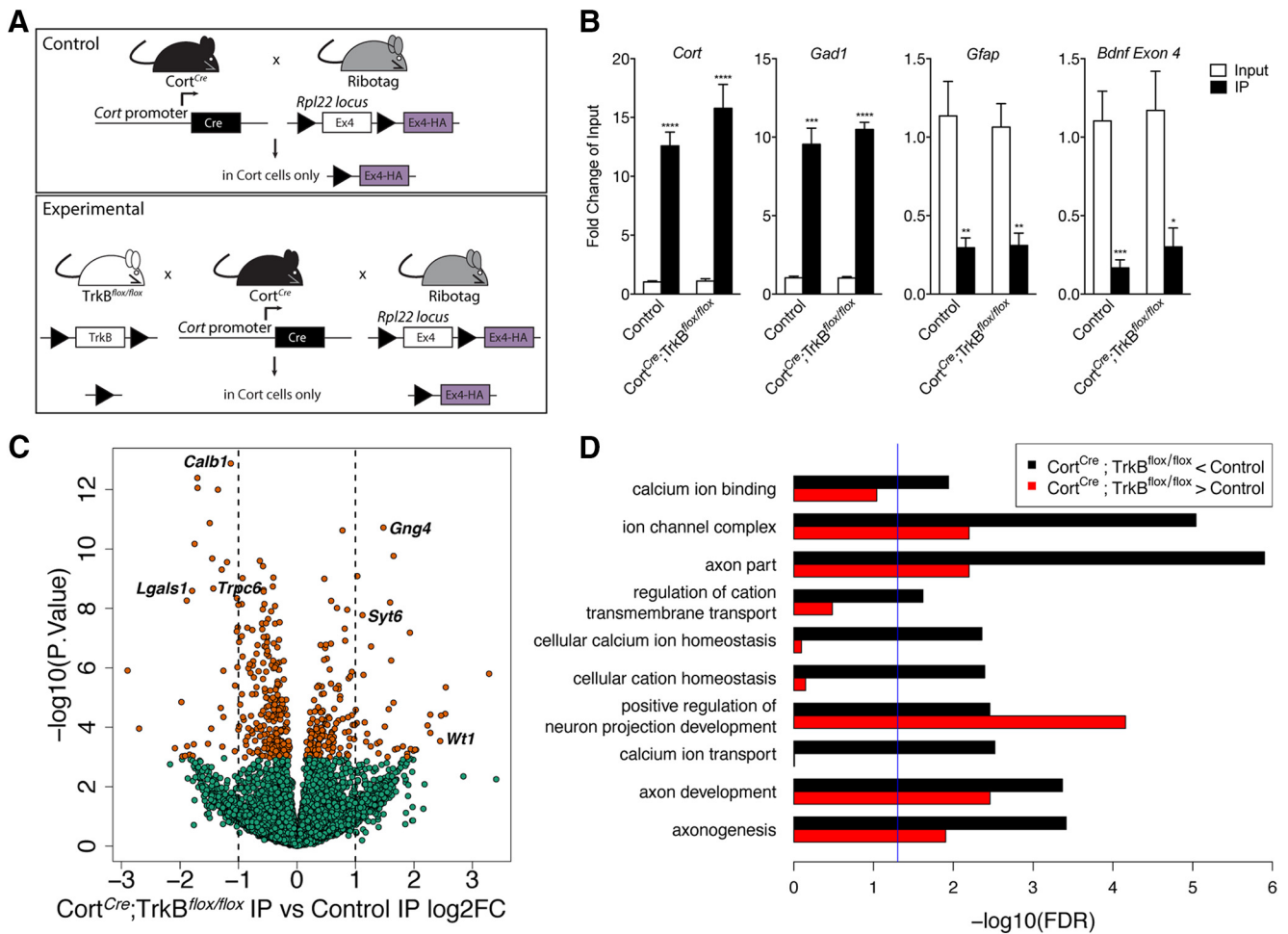


**Figure 3.** Loss of TrkB signaling in Cort neurons alters the expression of genes important for calcium homeostasis and axon development. **A**, Breeding strategy used to obtain control Cort<sup>Cre</sup>; Rpl22<sup>HA</sup> and experimental Cort<sup>Cre</sup>;TrkB<sup>flx/flx</sup>;Rpl22<sup>HA</sup> mice. **B**, Validation of Ribotag allele expression in cortistatin cells of control and Cort<sup>Cre</sup>;TrkB<sup>flx/flx</sup>;Rpl22<sup>HA</sup> mice by qPCR of *Cort* as well as *Gad*, *Gfap*, and *Bdnf* exon IV ( $n = 6$  per genotype, Student's unpaired  $t$  test; data are presented as the mean  $\pm$  SEM:  $*p < 0.05$ ,  $**p < 0.01$ ,  $***p < 0.001$ ,  $****p < 0.0001$  vs control). **C**, Volcano plot of RNA-seq results with Cort<sup>Cre</sup>;TrkB<sup>flx/flx</sup>;Rpl22<sup>HA</sup> IP versus Cort<sup>Cre</sup>;Rpl22<sup>HA</sup> IP log<sub>2</sub> fold change against  $-\log_{10} p$  value. Orange dots represent genes that are significantly different in Cort<sup>Cre</sup>;TrkB<sup>flx/flx</sup>;Rpl22<sup>HA</sup> IP versus Cort<sup>Cre</sup>;Rpl22<sup>HA</sup> IP, including *Wt1*, *Calb1*, *Lgals1*, *Trpc6*, *Syt6*, and *Gng4*. Green dots represent nonsignificant genes. See Extended Data Figure 3-1. **D**, GO terms in the molecular function, biological processes, and cellular component categories for genes enriched and de-enriched in Cort neurons following removal of TrkB and disruption of BDNF–TrkB signaling. See Extended Data Figures 3-2, 3-3, and 3-4.

hensive molecular profile of genes enriched and depleted in TrkB-deficient Cort neurons. Among the 21,187 expressed genes (at RPKM > 0.1), we identified 444 differentially expressed between IP RNA fractions at FDR < 0.05, including 75 genes with fold changes >2 (Fig. 3C, Extended Data Fig. 3-1). Of particular interest, differential expression analysis confirmed significant enrichment (Cort<sup>Cre</sup>; TrkB<sup>flx/flx</sup> IP compared with control IP) of Wilms tumor 1 (*Wt1*), synaptotagmin 6 (*Syt6*), and G-protein subunit gamma 4 (*Gng4*) transcripts (5.45-, 2.17-, and 2.78-fold increase,  $p = 2.91 \times 10^{-4}$ ,  $1.68 \times 10^{-8}$ ,  $1.9 \times 10^{-11}$ , respectively). We observed significant depletion of transcripts for the transient receptor potential cation channel subfamily C member 6 (*Trpc6*), calbindin 1 (*Calb1*), and galectin 1 (*Lgals1*) transcripts (1.3-, 2.69-, 2.19-, and 3.46-fold decrease,  $p = 2.93 \times 10^{-8}$ ,  $2.13 \times 10^{-9}$ ,  $1.3 \times 10^{-13}$ ,  $2.55 \times 10^{-9}$ , respectively). Several of

these genes are of interest due to their involvement in calcium signaling/homeostasis (Butz et al., 1999; Li et al., 2012; Schmidt, 2012) and axon development (Kobayakawa et al., 2015), pathways identified to be perturbed in bulk cortex following BDNF–TrkB disruption in Cort neurons (Fig. 1).

To explore the functional significance of the mRNAs enriched and depleted in Cort interneurons with disrupted BDNF–TrkB signaling, we performed GO analysis on the subset of 161 Entrez genes more highly expressed in TrkB-depleted Cort neurons and the 269 Entrez genes more highly expressed in control Cort neurons (Fig. 3D, Extended Data Fig. 3-2). Terms in both the molecular function and biological processes categories showed that cortistatin interneurons with disrupted BDNF–TrkB signaling were depleted for calcium ion binding, cellular calcium ion homeostasis, and calcium ion transport (FDR < 0.05).

ion channel complex and axon part, two cellular component category terms, were both depleted and enriched in *Cort<sup>Cre</sup>;TrkB<sup>flox/flox</sup>* interneurons, which indicates that disrupting BDNF–TrkB signaling modulates important cellular responses. For the biological process terms, positive regulation of neuron projection development and axon development were both enriched and depleted in those interneurons. Terms associated with both enrichment and depletion in *Cort* interneurons include different genes, which suggests that these cells may undergo gene-specific changes that support their ability to respond to different cellular signaling pathways. Together, these results support the hypothesis that BDNF–TrkB signaling regulates structural and functional plasticity in *Cort* interneurons to maintain excitatory/inhibitory balance.

To independently validate RNA-seq hits, we used qPCR to confirm significant enrichment and depletion of the above-mentioned transcripts in *Cort<sup>Cre</sup>;TrkB<sup>flox/flox</sup>* IP samples compared with control IP samples. We showed significant enrichment of *Wt1*, *Syt6*, and *Gng4* transcripts (3-, 2.8-, 2.9-fold changes,  $p < 0.01$ , 0.001, 0.0001, respectively). Furthermore, we showed significant depletion of *Trpc6*, *Calb1*, and *Lgals1* transcripts (0.3-, 0.5-, and 0.25-fold changes;  $p < 0.001$ , 0.001, 0.0001; Fig. 4A). We independently validated significant enrichment of *Wt1* using single-molecule fluorescence *in situ* hybridization in *TrkB*-ablated *Cort* neurons (*Cort<sup>Cre</sup>;TrkB<sup>flox/flox</sup>*) compared with control *Cort* neurons ( $p < 0.0001$ ; Fig. 4B–D).

### Genes important for *Cort* neuron identity and function overlap with those identified in autism spectrum disorder

Finally, we explored the potential clinical relevance of deficits in *Cort* neuron function using predefined genes sets from autism-sequencing studies [using Simons Foundation Autism Research Initiative (SFARI)] and disease ontologies (using Harmonizome). We found no significant enrichment in our bulk RNA-seq data with those identified in both autism spectrum disorder (ASD) and animal models relevant for ASD by the SFARI (Banerjee-Basu and Packer, 2010). However, we found enrichment for ASD genes among those genes highly expressed in *Cort* interneurons (Extended Data Fig. 3-3). For example, of the 239 genes in the “Mouse models” SFARI database expressed in our data, 27 (11.0%) were differentially expressed in *Cort* interneurons compared with total cortex, constituting a 6.3-fold enrichment ( $p = 9.25 \times 10^{-13}$ ). Similarly, of the 937 genes in the “Human gene” SFARI database (which contains genes with rare variations associated with ASD from sequencing studies) with homologs expressed in our data, 93 were differentially expressed (9.9%, 4.2-fold enrichment;  $p = 9.03 \times 10^{-25}$ ). These enrichments were preserved in the more stringent subset of ASD genes, either with [odds ratio (OR) = 5.71,  $p = 8.98 \times 10^{-14}$ ] or without (OR = 6.55,  $p = 8.06 \times 10^{-8}$ ) syndromic genes (see Materials and Methods). We further found significant enrichment for the overlap of genes differentially expressed in *TrkB*-depleted *Cort* cells compared with control *Cort* cells with those identified in

both human and animal models of ASD as identified by SFARI (Extended Data Fig. 3-3). Here, of the 237 genes in the Mouse models SFARI database expressed in our data, 26 (11.0%) were differentially expressed in *Cort<sup>Cre</sup>;TrkB<sup>flox/flox</sup>* mice compared with control, constituting a sixfold enrichment ( $p = 6.85 \times 10^{-12}$ ). Similarly, of the 917 genes in the Human gene SFARI database with homologs expressed in our data, 66 were differentially expressed (7.2%, 2.8-fold enrichment,  $p = 3.06 \times 10^{-11}$ ), which were preserved in the smaller subset of more stringent ASD genes with (OR = 2.83,  $p = 0.002$ ) or without (OR = 2.68,  $p = 0.02$ ) syndromic genes (see Materials and Methods).

In addition to the overlap of ASD-relevant genes with those important for *Cort* identity and function, there was significant enrichment of many gene sets related to psychiatric disorders (at both the diseases and endophenotype levels) in the Harmonizome database (Rouillard et al., 2016) with those sets of genes preferentially expressed in *Cort* neurons and those dysregulated following *TrkB* depletion (Extended Data Fig. 3-4). In addition to enrichment for psychiatric disorders, we further found enrichment of epilepsy-related genes among *TrkB*-depleted and control *Cort* neurons (35 genes,  $p = 1.93 \times 10^{-12}$ ; Extended Data Fig. 3-4). Together, these results further implicate *Cort* neurons in several debilitating human brain disorders (Xu et al., 2014).

## Discussion

### TrkB signaling in *Cort* interneurons regulates gene pathways that modulate cortical excitability

To better understand how disrupting BDNF–TrkB signaling in *Cort* cells impairs cortical function, we performed bulk RNA-seq on cortical tissue derived from *Cort<sup>Cre</sup>;TrkB<sup>flox/flox</sup>* and control mice and identified significant differential expression of genes important for excitatory neuron function. Pathway analysis of these differentially expressed genes revealed functions associated with glutamatergic synapses and synaptic membranes (Fig. 1C). For example, we observed altered expression of neuronal pentraxin II (*Nptx2*; log<sub>2</sub>FC = 1.26,  $p = 3.60 \times 10^{-5}$ ), which encodes a synaptic protein implicated in excitatory synapse formation and neural plasticity (Gu et al., 2013) that is bidirectionally regulated by BDNF in hippocampal neurons both *in vitro* and *in vivo* (Mariga et al., 2015). Our dataset also shows increases in cAMP-responsive element Binding Protein 3 Like 1, which is necessary and sufficient to activate *Nptx2* transcription after BDNF treatment (Mariga et al., 2015). The protein encoded by *Nptx2* is also directly implicated in BDNF-mediated modulation of glutamatergic synapses, where it facilitates targeting and stabilization of AMPA receptors on excitatory synapses (Chang et al., 2010; Martin and Finsterwald, 2011; Pelkey et al., 2015). *Npy* is another differentially expressed gene (log<sub>2</sub>FC = 0.75,  $p = 2.24 \times 10^{-5}$ ) that influences cortical excitability by reducing excitatory transmission onto neurons in the lateral habenula (Cheon et al., 2019) and inhibiting glutamatergic synaptic transmission in the hippocampus (Xapelli et al., 2008). NPY expression can slow the spread of seizures and has

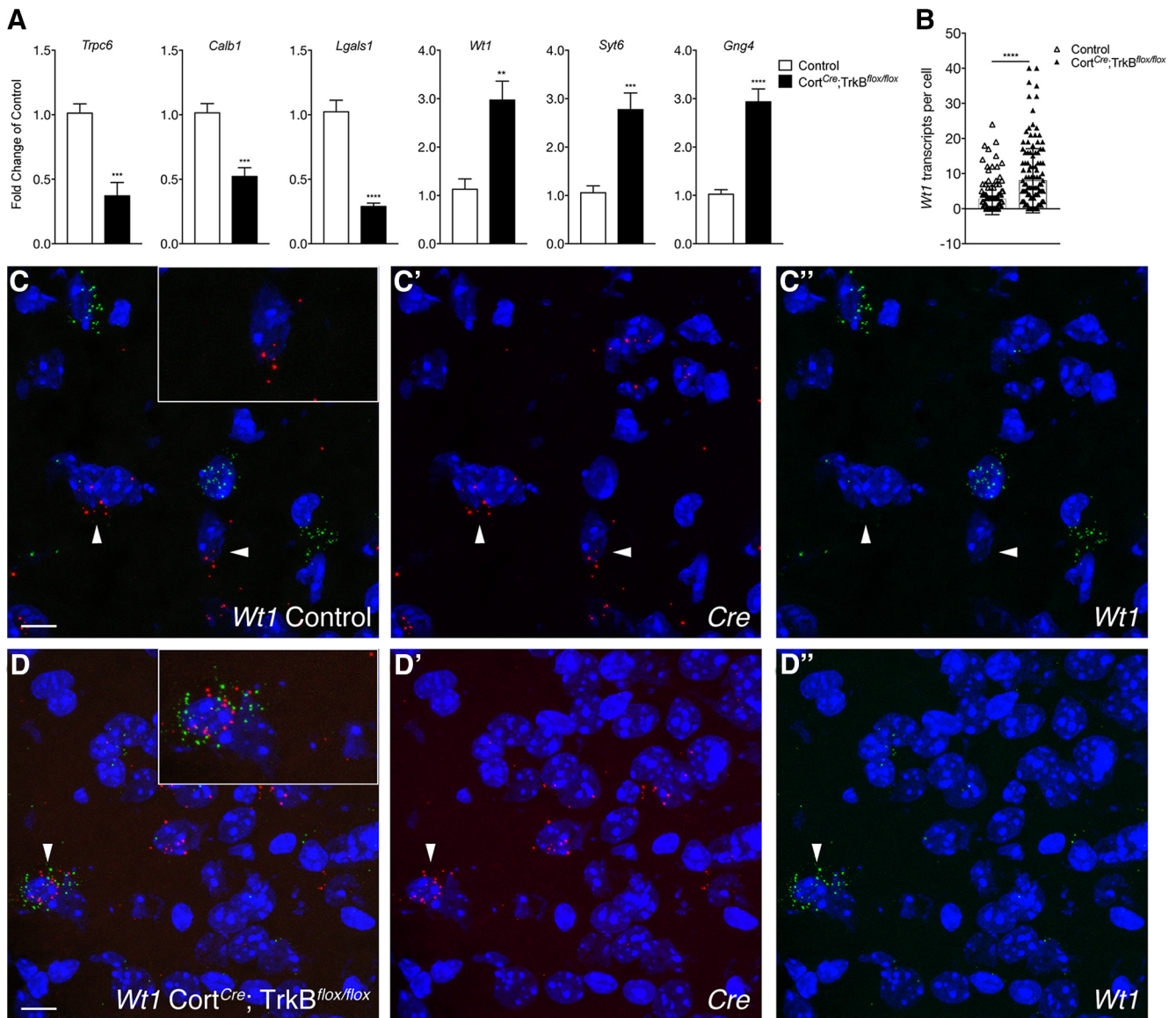


**Figure 4.** Validation of select targets from Control versus Cort<sup>Cre</sup>;TrkB<sup>flox/flox</sup> RNA-seq using qPCR and single-molecule fluorescence *in situ* hybridization. **A**, qPCR analysis validating select genes (*Trpc6*, *Calb1*, *Lgals1*, *Wt1*, *Syt6*, *Gng4*) found to be differentially expressed in Cort<sup>Cre</sup>;TrkB<sup>flox/flox</sup> IP versus control IP RNA-seq data ( $n = 6$  per genotype, Student's unpaired  $t$  test; data are presented as the mean  $\pm$  SEM: \*\* $p < 0.01$ , \*\*\* $p < 0.001$ , \*\*\*\* $p < 0.0001$  vs control). **B**, Quantification of *Wt1* transcripts in Cre positive cells of Cort<sup>Cre</sup>;TrkB<sup>flox/flox</sup> and control mice. **C**, **D**, Confocal z-projections of Cre and *Wt1* transcripts in the cortex from P21 Control (**C**) and Cort<sup>Cre</sup>;TrkB<sup>flox/flox</sup> (**D**) mice visualized with RNAscope *in situ* hybridization. *Wt1* transcripts (green) are more enriched in Cort neurons of Cort<sup>Cre</sup>;TrkB<sup>flox/flox</sup> than of Control mice. Inset depicts higher magnification of nuclei highlighted by arrows. Scale bars, **C**, **D**, 10  $\mu$ m.

neuroprotective effects against excitotoxicity via increased BDNF signaling (Richichi et al., 2004; Xapelli et al., 2008).

*Bdnf* transcripts are paradoxically upregulated when comparing Cort<sup>Cre</sup>;TrkB<sup>flox/flox</sup> to controls in the bulk RNA-seq dataset ( $\log_2FC = 0.95$ ,  $p = 3.55 \times 10^{-5}$ ). Because TrkB receptors were selectively depleted from Cort interneurons, which do not synthesize BDNF (Gorba and Wahle, 1999; Swanwick et al., 2004), *Bdnf* increases likely result from upregulation in cortical excitatory neurons. *Bdnf* expression may be induced in excitatory neurons following the loss of TrkB in Cort interneurons for several

reasons. First, in Cort<sup>Cre</sup>;TrkB<sup>flox/flox</sup> mice, impaired Cort interneuron function may facilitate disinhibition of excitatory neurons leading to increased cortical excitability and subsequent activity-induced *Bdnf* expression (Lu, 2003). Alternatively, increased *Bdnf* expression may be a compensatory mechanism attempting to counterbalance TrkB depletion in cortistatin cells. BDNF levels increase following seizures (Gall et al., 1991; Isackson et al., 1991; Mudò et al., 1996), and increases in BDNF can subsequently contribute to hyperexcitability and seizure propagation (Kokaia et al., 1995; Scharfman, 1997; Binder et al., 1999; Croll et al., 1999). Therefore, initiation and progres-

sive worsening of seizures seen in  $Cort^{Cre};TrkB^{flox/flox}$  mice could be exacerbated by increases in *Bdnf*. It should be noted that at the time of brain extraction (P21), mild seizures may have already begun and could be influencing gene expression. In summary, depletion of TrkB receptors from Cort inhibitory interneurons may disrupt inhibitory signaling, leading to disinhibition of cortical excitatory neurons and disruption of network activity. This imbalance may push the cortex toward elevated excitation and increased expression of activity-regulated genes such as *Bdnf*, *Nptx2*, and *Npy*.

### Cortistatin neurons are enriched in genes relevant to ASD

Translatome profiling in Cort neurons showed enrichment of neuron-relevant genes such as *Syt2*, a synaptic vesicle membrane protein (Bornschein and Schmidt, 2018) and *Nxph1*, a protein important for dendrite–axon adhesion (Born et al., 2014). We also observed expected depletion of genes such as *Mal*, which is implicated in myelination (Schaeren-Wiemers et al., 1995a), and *ApoE*, which is synthesized in astrocytes (Holtzman et al., 2012). These data expand on a similar translatome profiling experiment previously performed by Doyle et al. (2008) using different mouse models and methodology. In that study, investigators used a mouse in which the EGFP-L10a ribosomal fusion protein is expressed under control of the *Cort* promoter in a bacterial artificial chromosome, and gene expression data were obtained using a microarray approach combined with TRAP. Here, we used a mouse that expresses Cre from the endogenous *Cort* promoter, and gene expression data were obtained using a Ribotag/RNA-seq approach. Reassuringly, there is significant overlap between the Doyle microarray dataset and our RNA-seq analysis (Extended Data Fig. 2-1).

Xu et al. (2014) showed candidate autism genes from human genetics studies are enriched in Cort cells, supporting the notion that cortical interneurons play a significant role in the etiology of ASD. Epilepsy, a common neurologic disorder characterized by recurrent seizures, is highly comorbid with ASD (Viscidi et al., 2013), and it has been proposed that these disorders may have overlapping genetic risk that points to shared underlying molecular and cellular mechanisms. Of note, interneuron dysfunction has been identified as a potential shared cellular mechanism in mouse models of both disorders (Jacob, 2016). Our results further demonstrate enrichment of genes associated with epilepsy and ASD in Cort neurons and highlight differential expression of several ASD and epilepsy genes in Cort neurons following the disruption of TrkB signaling. Our findings support the overlapping developmental origins of the two illnesses and highlight BDNF–TrkB signaling as potentially relevant to their etiology.

### Genes associated with calcium signaling and axonal development are disrupted following TrkB depletion in cortistatin interneurons

To identify putative molecular mechanisms that contribute to Cort interneuron dysfunction in  $Cort^{Cre};TrkB^{flox/flox}$  mice, we compared the translomes of intact Cort

interneurons and Cort interneurons depleted of TrkB receptors. TrkB-depleted Cort neurons show dysregulation of genes associated with calcium ion homeostasis (*Calb1*, calcium binding protein; Schmidt, 2012) or calcium-dependent functions (*Syt6*, calcium dependent exocytosis; Fukuda et al., 2003), as well as genes associated with axon development (*Robo1*, axon guidance; Andrews et al., 2006) and cell–cell or cell–matrix interactions (*Lgals1*, plasma membrane adhesion molecule; Camby et al., 2006).

During development, cortical interneurons are generated in the ventral subcortical telencephalon and travel long distances to reach their final destination in cortical circuits, both tangentially from their birthplace in the ganglionic eminences and radially to their correct laminar position (Cooper, 2013). Chemokine signaling is important for the transition from tangential to radial migration, and the expression of chemokine receptors is directly affected by BDNF–TrkB signaling in the central nervous system, as well as in disease states such as cancer (Azoulay et al., 2018). We found that expression of *Cxcr4*, a chemokine receptor, is reduced in TrkB-depleted cortistatin interneurons by a factor of 4, which supports previous work showing modulation of CXCR4 expression and receptor internalization by BDNF–TrkB signaling (Ahmed et al., 2008). Degradation of this protein has been identified as a permissive signal for interneurons to leave tangential migratory streams (Sánchez-Alcañiz et al., 2011). Deletion of the gene leads to defects in cortical layer positioning (Li et al., 2008; Wang et al., 2011) and mutations result in premature accumulation of interneurons in the cortex. Although laminar distribution of Cort cells does not appear to be significantly altered by loss of TrkB (Hill et al., 2019), premature entry into the cortex may result in incorrect integration into the circuitry or improper axonal projections that cannot be inferred by laminar position. This explanation is further supported by altered expression of genes associated with axonogenesis, axon guidance, neuron projection terminus, and cell–matrix interactions (Fig. 3). The fact that CXCR4 is normally expressed in axons and functions to define their trajectory (Lieberam et al., 2005; Vilz et al., 2005; Miyasaka et al., 2007) provides additional strength to this hypothesis. In addition to *Cxcr4*, calcium signaling is important for stimulating (Behar et al., 1999) and halting (Bortone and Polleux, 2009) neuronal migration to the cortex, and  $Cort^{Cre};TrkB^{flox/flox}$  mice show decreased expression of genes in calcium-related GO categories compared with control mice (Fig. 3), such as *Calb1*. Importantly, exogenous application of BDNF induces the elevation of intracellular calcium (Berninger et al., 1993; Marsh and Palfrey, 1996), and endogenous BDNF signaling elicits calcium responses at synapses (Lang et al., 2007). Additional work would be necessary to tease out the effects of interneuron migration, migratory stream maintenance, and correct development of projections during embryonic development in these mutant mice. An important future direction will be to evaluate the morphology of Cort neurons following the disruption of BDNF–TrkB signaling.

In summary, we provide evidence that the loss of BDNF–TrkB signaling in Cort interneurons leads to alterations in calcium signaling and axon development in these cells, which may contribute to altered excitatory/inhibitory balance in the cortex. Several of the genes enriched in Cort neurons and differentially expressed in TrkB-depleted neurons are implicated in both ASD and epilepsy. These data shed light on the role of BDNF–TrkB signaling in the function of Cort-expressing interneurons and provide the rationale for further functional studies of these interneurons.

## References

- Ahmed F, Tessarollo L, Thiele C, Mocchetti I (2008) Brain-derived neurotrophic factor modulates expression of chemokine receptors in the brain. *Brain Res* 1227:1–11.
- Alcántara S, Pozas E, Ibañez CF, Soriano E (2006) BDNF-modulated spatial organization of Cajal-Retzius and GABAergic neurons in the marginal zone plays a role in the development of cortical organization. *Cereb Cortex* 16:487–499.
- Andrews W, Liapi A, Plachez C, Camurri L, Zhang J, Mori S, Murakami F, Parnavelas JG, Sundaresan V, Richards LJ (2006) Robo1 regulates the development of major axon tracts and interneuron migration in the forebrain. *Development* 133:2243–2252.
- Azoulay D, Herishanu Y, Shapiro M, Brandshaft Y, Surui C, Akría L, Braester A (2018) Elevated serum BDNF levels are associated with favorable outcome in CLL patients: possible link to CXCR4 down-regulation. *Exp Hematol* 63:17–21.e1.
- Banerjee-Basu S, Packer A (2010) SFARI Gene: an evolving database for the autism research community. *Dis Model Mech* 3:133–135.
- Baydyuk M, Russell T, Liao GY, Zang K, An JJ, Reichardt LF, Xu B (2011) TrkB receptor controls striatal formation by regulating the number of newborn striatal neurons. *Proc Natl Acad Sci U S A* 108:1669–1674.
- Behar TN, Scott CA, Greene CL, Wen X, Smith SV, Maric D, Liu QY, Colton CA, Barker JL (1999) Glutamate acting at NMDA receptors stimulates embryonic cortical neuronal migration. *J Neurosci* 19:4449–4461.
- Berninger B, García DE, Inagaki N, Hahnel C, Lindholm D (1993) BDNF and NT-3 induce intracellular Ca<sup>2+</sup> elevation in hippocampal neurones. *Neuroreport* 4:1303–1306.
- Binder DK, Routbort MJ, Ryan TE, Yancopoulos GD, McNamara JO (1999) Selective inhibition of kindling development by intraventricular administration of TrkB receptor body. *J Neurosci* 19:1424–1436.
- Born G, Breuer D, Wang S, Rohlmann A, Coulon P, Vakili P, Reissner C, Kiefer F, Heine M, Pape HC, Missler M (2014) Modulation of synaptic function through the  $\alpha$ -neurexin-specific ligand neurexophilin-1. *Proc Natl Acad Sci U S A* 111:E1274–E1283.
- Bornschein G, Schmidt H (2018) Synaptotagmin Ca(2+) sensors and their spatial coupling to presynaptic cav channels in central cortical synapses. *Front Mol Neurosci* 11:494.
- Bortone D, Polleux F (2009) KCC2 expression promotes the termination of cortical interneuron migration in a voltage-sensitive calcium-dependent manner. *Neuron* 62:53–71.
- Butz S, Fernandez-Chacon R, Schmitz F, Jahn R, Südhof TC (1999) The subcellular localizations of atypical synaptotagmins III and VI. Synaptotagmin III is enriched in synapses and synaptic plasma membranes but not in synaptic vesicles. *J Biol Chem* 274:18290–18296.
- Camby I, Le Mercier M, Lefranc F, Kiss R (2006) Galectin-1: a small protein with major functions. *Glycobiology* 16:137R–157R.
- Cellerino A, Maffei L, Domenici L (1996) The distribution of brain-derived neurotrophic factor and its receptor trkB in parvalbumin-containing neurons of the rat visual cortex. *Eur J Neurosci* 8:1190–1197.
- Chang MC, Park JM, Pelkey KA, Grabenstatter HL, Xu D, Linden DJ, Sutula TP, McBain CJ, Worley PF (2010) Narp regulates homeostatic scaling of excitatory synapses on parvalbumin-expressing interneurons. *Nat Neurosci* 13:1090–1097.
- Cheon M, Park H, Rhim H, Chung C (2019) Actions of neuropeptide Y on synaptic transmission in the lateral habenula. *Neuroscience* 410:183–190.
- Colliva A, Maynard KR, Martinowich K, Tongiorgi E (2018) Detecting single and multiple BDNF transcripts by in situ hybridization in neuronal cultures and brain sections, pp 1–27. New York: Humana.
- Cooper JA (2013) Cell biology in neuroscience: mechanisms of cell migration in the nervous system. *J Cell Biol* 202:725–734.
- Croll SD, Suri C, Compton DL, Simmons MV, Yancopoulos GD, Lindsay RM, Wiegand SJ, Rudge JS, Scharfman HE (1999) Brain-derived neurotrophic factor transgenic mice exhibit passive avoidance deficits, increased seizure severity and in vitro hyperexcitability in the hippocampus and entorhinal cortex. *Neuroscience* 93:1491–1506.
- Csaba Z, Dournaud P (2001) Cellular biology of somatostatin receptors. *Neuropeptides* 35:1–23.
- de Lecea L, Criado JR, Prospero-Garcia O, Gautvik KM, Schweitzer P, Danielson PE, Dunlop CL, Siggins GR, Henriksen SJ, Sutcliffe JG (1996) A cortical neuropeptide with neuronal depressant and sleep-modulating properties. *Nature* 381:242–245.
- de Lecea L, del Rio JA, Criado JR, Alcántara S, Morales M, Danielson PE, Henriksen SJ, Soriano E, Sutcliffe JG (1997) Cortistatin is expressed in a distinct subset of cortical interneurons. *J Neurosci* 17:5868–5880.
- Doyle JP, Dougherty JD, Heiman M, Schmidt EF, Stevens TR, Ma G, Bupp S, Shrestha P, Shah RD, Doughty ML, Gong S, Greengard P, Heintz N (2008) Application of a translational profiling approach for the comparative analysis of CNS cell types. *Cell* 135:749–762.
- Fukuda M, Kanno E, Ogata Y, Saegusa C, Kim T, Loh YP, Yamamoto A (2003) Nerve growth factor-dependent sorting of synaptotagmin IV protein to mature dense-core vesicles that undergo calcium-dependent exocytosis in PC12 cells. *J Biol Chem* 278:3220–3226.
- Gall C, Lauterborn J, Bundman M, Murray K, Isackson P (1991) Seizures and the regulation of neurotrophic factor and neuropeptide gene expression in brain. *Epilepsy Res Suppl* 4:225–245.
- Glorioso C, Sabatini M, Unger T, Hashimoto T, Monteggia LM, Lewis DA, Mirnics K (2006) Specificity and timing of neocortical transcriptome changes in response to BDNF gene ablation during embryogenesis or adulthood. *Mol Psychiatry* 11:633–648.
- Gorba T, Wahle P (1999) Expression of TrkB and TrkC but not BDNF mRNA in neurochemically identified interneurons in rat visual cortex in vivo and in organotypic cultures. *Eur J Neurosci* 11:1179–1190.
- Grishanin RN, Yang H, Liu X, Donohue-Rolfé K, Nune GC, Zang K, Xu B, Duncan JL, Lavail MM, Copenhagen DR, Reichardt LF (2008) Retinal TrkB receptors regulate neural development in the inner, but not outer, retina. *Mol Cell Neurosci* 38:431–443.
- Gu Y, Huang S, Chang MC, Worley P, Kirkwood A, Quinlan EM (2013) Obligatory role for the immediate early gene NARP in critical period plasticity. *Neuron* 79:335–346.
- Guilloux JP, Douillard-Guilloux G, Kota R, Wang X, Gardier AM, Martinowich K, Tseng GC, Lewis DA, Sibille E (2012) Molecular evidence for BDNF- and GABA-related dysfunctions in the amygdala of female subjects with major depression. *Mol Psychiatry* 17:1130–1142.
- Habib N, Avraham-David I, Basu A, Burks T, Shekhar K, Hofree M, Choudhury SR, Aguet F, Gelfand E, Ardlie K, Weitz DA, Rozenblatt-Rosen O, Zhang F, Regev A (2017) Massively parallel single-nucleus RNA-seq with DroNc-seq. *Nat Methods* 14:955–958.
- Hill JL, Jimenez DV, Mai Y, Ren M, Hallock HL, Maynard KR, Chen HY, Hardy NF, Schloesser RJ, Maher BJ, Yang F, Martinowich K (2019) Cortistatin-expressing interneurons require TrkB signaling to suppress neural hyper-excitability. *Brain Struct Funct* 224:471–483.

- Ho PW, Pang SY, Li M, Tse ZH, Kung MH, Sham PC, Ho SL (2015) PMCA4 (ATP2B4) mutation in familial spastic paraplegia causes delay in intracellular calcium extrusion. *Brain Behav* 5:e00321.
- Hodneland E, Kögel T, Frei DM, Gerdes HH, Lundervold A (2013) CellSegm - a MATLAB toolbox for high-throughput 3D cell segmentation. *Source Code Biol Med* 8:16.
- Hol EM, Pekny M (2015) Glial fibrillary acidic protein (GFAP) and the astrocyte intermediate filament system in diseases of the central nervous system. *Curr Opin Cell Biol* 32:121–130.
- Holtzman DM, Herz J, Bu G (2012) Apolipoprotein E and apolipoprotein E receptors: normal biology and roles in Alzheimer disease. *Cold Spring Harb Perspect Med* 2:a006312.
- Huang ZJ, Kirkwood A, Pizzorusso T, Porciatti V, Morales B, Bear MF, Maffei L, Tonegawa S (1999) BDNF regulates the maturation of inhibition and the critical period of plasticity in mouse visual cortex. *Cell* 98:739–755.
- Isackson PJ, Huntsman MM, Murray KD, Gall CM (1991) BDNF mRNA expression is increased in adult rat forebrain after limbic seizures: temporal patterns of induction distinct from NGF. *Neuron* 6:937–948.
- Jacob J (2016) Cortical interneuron dysfunction in epilepsy associated with autism spectrum disorders. *Epilepsia* 57:182–193.
- Karagiannis A, Gallopini T, David C, Battaglia D, Geoffroy H, Rossier J, Hillman EM, Staiger JF, Cauli B (2009) Classification of NPY-expressing neocortical interneurons. *J Neurosci* 29:3642–3659.
- Kasen S, Ouellette R, Cohen P (1990) Mainstreaming and postsecondary educational and employment status of a rubella cohort. *Am Ann Deaf* 135:22–26.
- Katoh-Semba R, Takeuchi IK, Semba R, Kato K (1997) Distribution of brain-derived neurotrophic factor in rats and its changes with development in the brain. *J Neurochem* 69:34–42.
- Kim D, Langmead B, Salzberg SL (2015) HISAT: a fast spliced aligner with low memory requirements. *Nat Methods* 12:357–360.
- Kobayakawa Y, Sakumi K, Kajitani K, Kadoya T, Horie H, Kira J, Nakabeppu Y (2015) Galectin-1 deficiency improves axonal swelling of motor neurons in SOD1(G93A) transgenic mice. *Neuropathol Appl Neurobiol* 41:227–244.
- Kokaia M, Erfors P, Kokaia Z, Elmér E, Jaenisch R, Lindvall O (1995) Suppressed epileptogenesis in BDNF mutant mice. *Exp Neurol* 133:215–224.
- Kuryatov A, Gerzanich V, Nelson M, Olale F, Lindstrom J (1997) Mutation causing autosomal dominant nocturnal frontal lobe epilepsy alters Ca<sup>2+</sup> permeability, conductance, and gating of human  $\alpha 4\beta 2$  nicotinic acetylcholine receptors. *J Neurosci* 17:9035–9047.
- Lang SB, Stein V, Bonhoeffer T, Lohmann C (2007) Endogenous brain-derived neurotrophic factor triggers fast calcium transients at synapses in developing dendrites. *J Neurosci* 27:1097–1105.
- Law CW, Chen Y, Shi W, Smyth GK (2014) voom: precision weights unlock linear model analysis tools for RNA-seq read counts. *Genome Biol* 15:R29.
- Li G, Adesnik H, Li J, Long J, Nicoll RA, Rubenstein JL, Pleasure SJ (2008) Regional distribution of cortical interneurons and development of inhibitory tone are regulated by Cxcl12/Cxcr4 signaling. *J Neurosci* 28:1085–1098.
- Li H, Huang J, Du W, Jia C, Yao H, Wang Y (2012) TRPC6 inhibited NMDA receptor activities and protected neurons from ischemic excitotoxicity. *J Neurochem* 123:1010–1018.
- Liao Y, Smyth GK, Shi W (2014) featureCounts: an efficient general purpose program for assigning sequence reads to genomic features. *Bioinformatics* 30:923–930.
- Lieberam I, Agalliu D, Nagasawa T, Ericson J, Jessell TM (2005) A Cxcl12-CXCR4 chemokine signaling pathway defines the initial trajectory of mammalian motor axons. *Neuron* 47:667–679.
- Lu B (2003) BDNF and activity-dependent synaptic modulation. *Learn Mem* 10:86–98.
- Mariga A, Glaser J, Mathias L, Xu D, Xiao M, Worley P, Ninan I, Chao MV (2015) Definition of a bidirectional activity-dependent pathway involving BDNF and Narp. *Cell Rep* 13:1747–1756.
- Marsh HN, Palfrey HC (1996) Neurotrophin-3 and brain-derived neurotrophic factor activate multiple signal transduction events but are not survival factors for hippocampal pyramidal neurons. *J Neurochem* 67:952–963.
- Martin JL, Finsterwald C (2011) Cooperation between BDNF and glutamate in the regulation of synaptic transmission and neuronal development. *Integr Biol (Camb)* 4:14–16.
- Martinowich K, Schloesser RJ, Jimenez DV, Weinberger DR, Lu B (2011) Activity-dependent brain-derived neurotrophic factor expression regulates corticostatin-interneurons and sleep behavior. *Mol Brain* 4:11.
- Marty S, Berninger B, Carroll P, Thoenen H (1996) GABAergic stimulation regulates the phenotype of hippocampal interneurons through the regulation of brain-derived neurotrophic factor. *Neuron* 16:565–570.
- Mátés L, Korpos E, Déak F, Liu Z, Beier DR, Aszódi A, Kiss I (2002) Comparative analysis of the mouse and human genes (Matn2 and MATN2) for matrilin-2, a filament-forming protein widely distributed in extracellular matrices. *Matrix Biol* 21:163–174.
- Meyer HS, Schwarz D, Wimmer VC, Schmitt AC, Kerr JN, Sakmann B, Helmstaedter M (2011) Inhibitory interneurons in a cortical column form hot zones of inhibition in layers 2 and 5A. *Proc Natl Acad Sci U S A* 108:16807–16812.
- Miyasaka N, Knaut H, Yoshihara Y (2007) Cxcl12/Cxcr4 chemokine signaling is required for placode assembly and sensory axon pathfinding in the zebrafish olfactory system. *Development* 134:2459–2468.
- Mudò G, Jiang XH, Timmusk T, Bindoni M, Belluardo N (1996) Change in neurotrophins and their receptor mRNAs in the rat forebrain after status epilepticus induced by pilocarpine. *Epilepsia* 37:198–207.
- Myers AJ, Gibbs JR, Webster JA, Rohrer K, Zhao A, Marlowe L, Kaleem M, Leung D, Bryden L, Nath P, Zismann VL, Joshipura K, Huentelman MJ, Hu-Lince D, Coon KD, Craig DW, Pearson JV, Holmans P, Heward CB, Reiman EM, et al. (2007) A survey of genetic human cortical gene expression. *Nat Genet* 39:1494–1499.
- Nieto-Gonzalez JL, Jensen K (2013) BDNF depresses excitability of parvalbumin-positive interneurons through an M-like current in rat dentate gyrus. *PloS One* 8:e67318.
- O'Brien RJ, Xu D, Petralia RS, Steward O, Hagan RL, Worley P (1999) Synaptic clustering of AMPA receptors by the extracellular immediate-early gene product Narp. *Neuron* 23:309–323.
- Ozawa H, Takata K (1995) The granin family—its role in sorting and secretory granule formation. *Cell Struct Funct* 20:415–420.
- Pang ZP, Melicoff E, Padgett D, Liu Y, Teich AF, Dickey BF, Lin W, Adachi R, Sudhof TC (2006) Synaptotagmin-2 is essential for survival and contributes to Ca<sup>2+</sup> triggering of neurotransmitter release in central and neuromuscular synapses. *J Neurosci* 26:13493–13504.
- Pelkey KA, Barksdale E, Craig MT, Yuan X, Sukumaran M, Vargish GA, Mitchell RM, Wyeth MS, Petralia RS, Chittajallu R, Karlsson RM, Cameron HA, Murata Y, Colonnese MT, Worley PF, McBain CJ (2015) Pentraxins coordinate excitatory synapse maturation and circuit integration of parvalbumin interneurons. *Neuron* 85:1257–1272.
- Pruunsild P, Timmusk T (2005) Structure, alternative splicing, and expression of the human and mouse KCNIP gene family. *Genomics* 86:581–593.
- Richichi C, Lin EJ, Stefanin D, Colella D, Ravizza T, Grignaschi G, Veglianesi P, Sperk G, During MJ, Vezzani A (2004) Anticonvulsant and anti-epileptogenic effects mediated by adeno-associated virus vector neuropeptide Y expression in the rat hippocampus. *J Neurosci* 24:3051–3059.
- Ritchie ME, Phipson B, Wu D, Hu Y, Law CW, Shi W, Smyth GK (2015) limma powers differential expression analyses for RNA-seq and microarray studies. *Nucleic Acids Res* 43:e47.
- Rouillard AD, Gundersen GW, Fernandez NF, Wang Z, Monteiro CD, McDermott MG, Ma'ayan A (2016) The harmonizome: a collection of processed datasets gathered to serve and mine knowledge about genes and proteins. *Database (Oxford)* 2016:baw100.

- Sánchez-Alcañiz JA, Haegel S, Mueller W, Pla R, Mackay F, Schulz S, López-Bendito G, Stumm R, Marín O (2011) Cxcr7 controls neuronal migration by regulating chemokine responsiveness. *Neuron* 69:77–90.
- Sanz E, Yang L, Su T, Morris DR, McKnight GS, Amieux PS (2009) Cell-type-specific isolation of ribosome-associated mRNA from complex tissues. *Proc Natl Acad Sci U S A* 106:13939–13944.
- Sanz E, Evanoff R, Quintana A, Evans E, Miller JA, Ko C, Amieux PS, Griswold MD, McKnight GS (2013) RiboTag analysis of actively translated mRNAs in Sertoli and Leydig cells in vivo. *PLoS One* 8:e66179.
- Sasi M, Vignoli B, Canossa M, Blum R (2017) Neurobiology of local and intercellular BDNF signaling. *Pflugers Arch* 469:593–610.
- Schaeren-Wiemers N, Valenzuela DM, Frank M, Schwab ME (1995a) Characterization of a rat gene, rMAL, encoding a protein with four hydrophobic domains in central and peripheral myelin. *J Neurosci* 15:5753–5764.
- Schaeren-Wiemers N, Schaefer C, Valenzuela DM, Yancopoulos GD, Schwab ME (1995b) Identification of new oligodendrocyte- and myelin-specific genes by a differential screening approach. *J Neurochem* 65:10–22.
- Scharfman HE (1997) Hyperexcitability in combined entorhinal/hippocampal slices of adult rat after exposure to brain-derived neurotrophic factor. *J Neurophysiol* 78:1082–1095.
- Schmidt H (2012) Three functional facets of calbindin D-28k. *Front Mol Neurosci* 5:25.
- Schweitzer P, Madamba SG, Siggins GR (2003) The sleep-modulating peptide cortistatin augments the h-current in hippocampal neurons. *J Neurosci* 23:10884–10891.
- Somogyi J, Baude A, Omori Y, Shimizu H, El Mestikawy S, Fukaya M, Shigemoto R, Watanabe M, Somogyi P (2004) GABAergic basket cells expressing cholecystokinin contain vesicular glutamate transporter type 3 (VGLUT3) in their synaptic terminals in hippocampus and isocortex of the rat. *Eur J Neurosci* 19:552–569.
- Souza-Moreira L, Morell M, Delgado-Maroto V, Pedreño M, Martínez-Escudero L, Caro M, O'Valle F, Luque R, Gallo M, de Lecea L, Castaño JP, Gonzalez-Rey E (2013) Paradoxical effect of cortistatin treatment and its deficiency on experimental autoimmune encephalomyelitis. *J Immunol* 191:2144–2154.
- Svenningsson P, Kim Y, Warner-Schmidt J, Oh YS, Greengard P (2013) p11 and its role in depression and therapeutic responses to antidepressants. *Nat Rev Neurosci* 14:673–680.
- Swanwick CC, Harrison MB, Kapur J (2004) Synaptic and extrasynaptic localization of brain-derived neurotrophic factor and the tyrosine kinase B receptor in cultured hippocampal neurons. *J Comp Neurol* 478:405–417.
- Taniguchi H, He M, Wu P, Kim S, Paik R, Sugino K, Kvitsiani D, Fu Y, Lu J, Lin Y, Miyoshi G, Shima Y, Fishell G, Nelson SB, Huang ZJ (2011) A resource of Cre driver lines for genetic targeting of GABAergic neurons in cerebral cortex. *Neuron* 71:995–1013.
- Tolppanen AM, Helisalmi S, Hiltunen M, Kolehmainen M, Schwab U, Pirttilä T, Pulkkinen L, Uusitupa M, Soininen H (2011) Tenomodulin variants, APOE and Alzheimer's disease in a Finnish case-control cohort. *Neurobiol Aging* 32:546.e7–9.
- Tremblay R, Lee S, Rudy B (2016) GABAergic interneurons in the neocortex: from cellular properties to circuits. *Neuron* 91:260–292.
- van Diessen E, Senders J, Jansen FE, Boersma M, Bruining H (2015) Increased power of resting-state gamma oscillations in autism spectrum disorder detected by routine electroencephalography. *Eur Arch Psychiatry Clin Neurosci* 265:537–540.
- Veber DF, Holly FW, Nutt RF, Bergstrand SJ, Brady SF, Hirschmann R, Glitzer MS, Saperstein R (1979) Highly active cyclic and bicyclic somatostatin analogues of reduced ring size. *Nature* 280:512–514.
- Vilz TO, Moepps B, Engele J, Molly S, Littman DR, Schilling K (2005) The SDF-1/CXCR4 pathway and the development of the cerebellar system. *Eur J Neurosci* 22:1831–1839.
- Viscidi EW, Triche EW, Pescosolido MF, McLean RL, Joseph RM, Spence SJ, Morrow EM (2013) Clinical characteristics of children with autism spectrum disorder and co-occurring epilepsy. *PLoS One* 8:e67797.
- Wang J, Barstein J, Ethridge LE, Mosconi MW, Takarae Y, Sweeney JA (2013) Resting state EEG abnormalities in autism spectrum disorders. *J Neurodev Disord* 5:24.
- Wang Y, Li G, Stanco A, Long JE, Crawford D, Potter GB, Pleasure SJ, Behrens T, Rubenstein JL (2011) CXCR4 and CXCR7 have distinct functions in regulating interneuron migration. *Neuron* 69:61–76.
- Xapelli S, Bernardino L, Ferreira R, Grade S, Silva AP, Salgado JR, Cavadas C, Grouzmann E, Poulsen FR, Jakobsen B, Oliveira CR, Zimmer J, Malva JO (2008) Interaction between neuropeptide Y (NPY) and brain-derived neurotrophic factor in NPY-mediated neuroprotection against excitotoxicity: a role for microglia. *Eur J Neurosci* 27:2089–2102.
- Xu X, Wells AB, O'Brien DR, Nehorai A, Dougherty JD (2014) Cell type-specific expression analysis to identify putative cellular mechanisms for neurogenetic disorders. *J Neurosci* 34:1420–1431.
- Yamada MK, Nakanishi K, Ohba S, Nakamura T, Ikegaya Y, Nishiyama N, Matsuki N (2002) Brain-derived neurotrophic factor promotes the maturation of GABAergic mechanisms in cultured hippocampal neurons. *J Neurosci* 22:7580–7585.
- Yu G, Wang LG, Han Y, He QY (2012) clusterProfiler: an R package for comparing biological themes among gene clusters. *OMICS* 16:284–287.
- Zhou Y, Danbolt NC (2014) Glutamate as a neurotransmitter in the healthy brain. *J Neural Transm (Vienna)* 121:799–817.